

Novel examples of cluster-matter produced by LUCAS, a new laser cluster source

M. Gartz^a, C. Keutgen, S. Kuenneke, and U. Kreibig

I. Physikalisches Institut der RWTH, D-52056 Aachen, Germany

Received: 1 September 1998 / Received in final form: 10 November 1998

Abstract. We present experimental results obtained by a novel cluster source, LUCAS, based on laser ablation/evaporation of high cluster yield. Deposition rates of ≈ 10 nm/s can be achieved for a broad field of materials. Experiments on three different examples of cluster-matter are presented. (1) Iron clusters ($2R = 20$ nm) are embedded in fullerite and compared to silver clusters ($2R = 2.6$ nm) where previously static and dynamic charge transfer has been detected [1]. (2) The chemical reactions of Y clusters ($2R = 16$ nm) with hydrogen and oxygen exhibit reversible and non-reversible structural and electronic phase transitions. (3) Crystalline ITO clusters are produced in nanoporous optical films (thickness 190 nm) with high conductivity and good stability.

PACS. 71.30.+h Metal-insulator transitions and other electronic transitions – 73.61.Tm Nanocrystalline materials – 78.66.-w Optical properties of specific thin films, surfaces, and low-dimensional structures

1 Introduction

To produce cluster beams and cluster-matter systems containing solid state clusters of materials with high melting temperatures and low vapor pressures, we developed the novel type of laser ablation and evaporation cluster source LUCAS (Laser Universal Cluster Ablation/Evaporation Source). It can be used for a broad field of metallic, semi-conducting and dielectric, elemental and compound materials, depending on the choice of laser, applied. The main purpose was to obtain high cluster yields. Details of the apparatus will be described elsewhere. In the following we present three application examples: metallic clusters in fullerite (Sect. 2), Yttrium clusters (Sect. 3) and ITO cluster films (Sect. 4). After producing and depositing the systems on a substrate under UHV conditions the optical extinction was measured between $1 \text{ eV} \leq \hbar\omega \leq 5 \text{ eV}$. The cluster systems were characterized by transmission electron microscopy yielding the size distributions of the nanoparticles.

2 Interface effects in nanostructured matter: static and dynamic charge transfer

We recently observed [1] that, by embedding metal clusters into solid or liquid host media, *both static and dynamic*

electron transfer can occur between the cluster and states of the surrounding layer of matrix material. Often, the host exhibits a broad distribution of interface influenced electronic (adsorbate like) states in the cluster/matrix interface region which depends on its chemical nature.

(1) *The static charge transfer* is caused to obtain *equilibration of the chemical potential* in the composite system and fills all host levels up to the resulting cluster Fermi level E_{Fermi} , forming an electric double layer in the interface. Thus, the conduction electron density of the clusters is influenced.

The optical absorption of many solid state metallic clusters is dominated by the Mie cluster plasmon excitation. Its peak energy $\hbar\omega_{\text{max}}$ depends on the conduction electron density N [2]. Changes of N can, hence, be determined directly from observed plasmon peak shifts.

(2) *The dynamic charge transfer* concerns electrons above E_{Fermi} which can pass over between cluster and interface electronic levels or (if an interface barrier exists) can tunnel through this barrier. After some *residence time* these electrons return back, and such alternating processes induce fluctuations in N proportional to the inverse cluster radius, R^{-1} .

We assume these latter processes to reduce the life-time of Mie cluster plasmons.

Adopting the model of the plasmon relaxation to be caused by sequences of statistical single electron events, we assume the dynamic charge transfer processes to con-

^a Corresponding author.

e-mail: gartz@physik.rwth-aachen.de

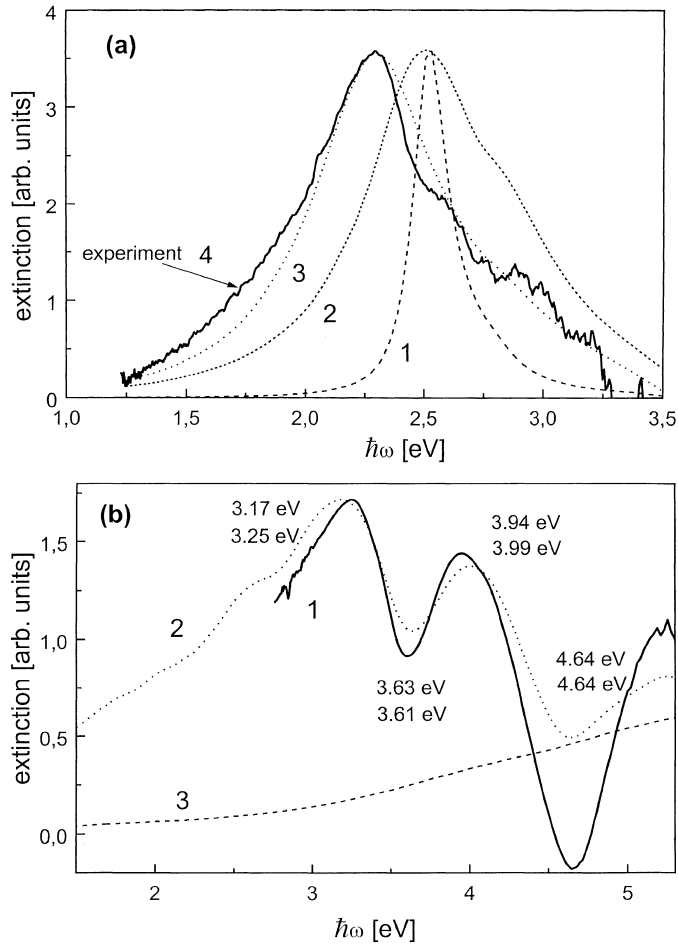


Fig. 1. (a) Optical extinction spectra of 2.6 nm Ag clusters in fullerite (fullerite reference subtracted): 1 Mie theory, $A = 0$; 2 Mie theory (absorbing matrix), $A = 1$, $\Delta N = 0$; 3 Mie theory (absorbing matrix), $A = 1$, $\Delta N/N = -20\%$; 4 measured extinction of the Ag clusters. (b) 20 nm Fe clusters in fullerite (fullerite reference subtracted): 1 measured extinction of the sample; 2 Mie theory (absorbing matrix); 3: Mie theory for free Fe clusters.

tribute to the *dephasing relaxation* of the collective excitation which is due to the energy quantized, coherent, *collective drift motion*.

I.e., electrons, performing a charge transfer back and forth through the interface, lose their phase of the collective drift motion. Within this model, the dephasing relaxation can be led back to single Drude electron relaxation processes, the frequency of which is known to follow the dependence $\gamma(R) = \gamma^{\text{bulk}} + v_{\text{Fermi}}A/R$ [2] where the second term includes *cluster size* and *surface effects*.

The A -parameter, describing, beside contributions of quantum size effects, the effectivity and frequency of single electron relaxation events at the surface, is, hence, a measure of the cluster plasmon dephasing relaxation and its changes due to the material surrounding the cluster. It contains information about electronic cluster-matrix interface states. Since the plasmon band width Γ follows $\Gamma^{\text{exp}} - \Gamma_{\text{Mie}}^{\text{bulk}} \propto (A/R)$ [2], the A pa-

rameter can be determined directly from measured band widths.

For *free* jellium clusters the quantum size effect yields $A \approx 0.3$ [10]. After *embedding* the clusters, additional contributions arise from the *dynamic charge transfer* processes, hence, A increases.

In the experiments presented here, we selected solid fullerite as embedding medium for silver clusters (2.6 ± 0.3 nm) produced as described in [1] and for iron clusters (20 ± 8 nm) produced by LUCAS. In Fig. 1a and 1b we compare their optical extinction spectra with spectra calculated from Mie's theory (extended to absorbing host [11] because C_{60} strongly absorbs in the VIS).

Ad (1) *Static charge transfer*: The shift between measured and calculated Mie peak in the Ag/ C_{60} -system (Fig. 1a) indicates a reduction of $\Delta N/N \approx -20\%$ [1]. Roughly, each C_{60} molecule in *direct* contact with the silver surface takes *one* electron. We interpret this effect as the formation of a charge double layer in the interface region. In film systems similar results were found earlier from ESCA experiments [3].

The complementary indication of the excess electrons in the C_{60} interface layer was obtained from the Fe/ C_{60} -system which was produced by the novel laser cluster machine LUCAS.

It is expected that *iron clusters* act as donors like silver when embedded in fullerite. Since, in contrast to silver, *free* iron clusters do not exhibit any spectrally selective absorption features like a Mie plasmon resonance, in the VIS, the observed *selective* changes in the optical transmission (Fig. 1b) compared to the calculated Mie-spectrum (including host absorption [11]) are ascribed to occupation of levels in the *interface- C_{60}* by transfer electrons from the metal cluster and energy changes of these levels. A quantitative analysis is still pending.

Summarizing, *the static charge transfer* was indicated, both, by the lack of electrons in the metal clusters in the system Ag/ C_{60} and by excess electrons in the fullerite interface in the system Fe/ C_{60} .

Ad (2) *Dynamic charge transfer*: Comparing the Mie *band widths* measured and calculated for the Ag/ C_{60} -system, we observe drastic increase in the experimental spectra. We ascribe it to the *dynamic charge transfer* and the resulting increase in *dephasing relaxation* of the plasmon excitation. We find an A -parameter of $A = 1$ (Fig. 1a), in good agreement with findings from various other embedding media [1].

The width of the Mie plasmon band of silver clusters results from complex interplay of damping and dispersion of the polarization [1]. Modeling, roughly, the measured Mie bands of *same* Ag-clusters in the free beam and in the fullerite matrix by Lorentzians (neglecting polarization dispersion effects and possible effects of inhomogeneous line broadening), we derived the *dephasing relaxation time* τ_d to amount to 7 fs for the clusters in the free beam (i.e. with clean surface) and to be reduced to $\tau_d \approx 3$ fs in the fullerite host [1]. Extrapolating to *free* 15 nm clusters we obtain $\tau_d \approx 20$ fs, not in contradiction to recent results of fs-spectroscopy [4, 5].

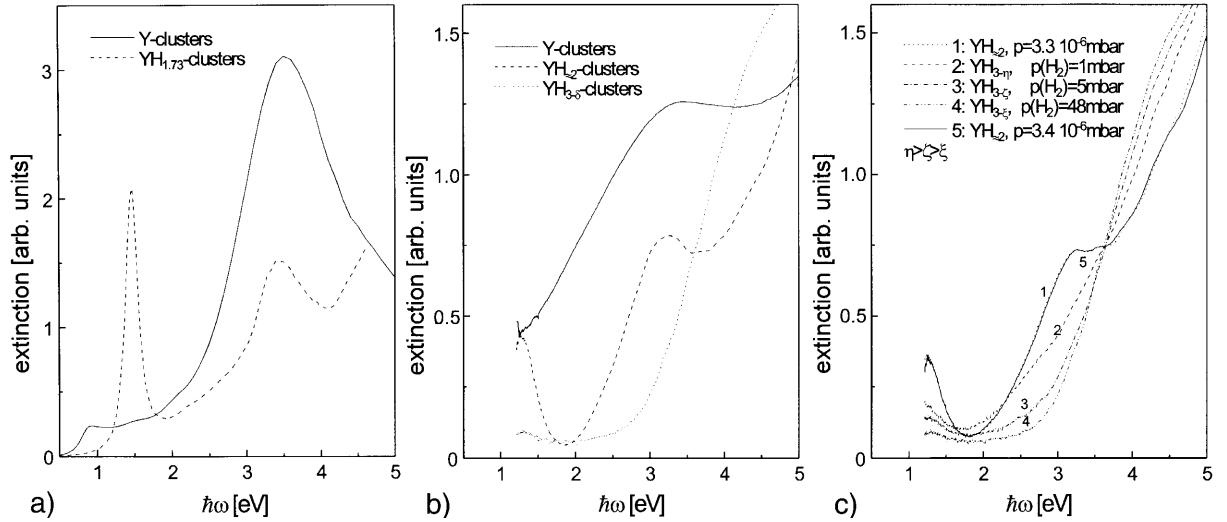
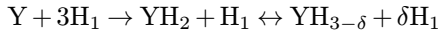


Fig. 2. (a) Mie calculations of the extinction cross sections of Y and $\text{YH}_{1.73}$ -clusters. (b) In-situ measurements of the extinction of Y, $\text{YH}_{\approx 2}$ and $\text{YH}_{3-\delta}$ -clusters. (c) Consecutive in situ measurements of the extinction during the $\text{YH}_2 \rightarrow \text{YH}_{3-\delta}$ reaction. The transition is completely reversible as can be recognized by the first (1) and the last (5) curve.

3 Reversible and non-reversible chemical reactions of Yttrium clusters

3.1 The reversible reaction $\text{YH}_2 \rightarrow \text{YH}_{3-\delta}$

It is well known [6] that the hydrogenation of Y films follows the reaction sequence [7]



The most striking effect is that YH_2 is metallic with fcc structure while $\text{YH}_{3-\delta}$ shows semiconducting behaviour and hcp structure where the band gap is enlarged with decreasing δ . In experiments, the gap energy of 1.8 eV was found for $\delta = 0.2$ [6].

Hence, increasing the H_1 gas pressure and/or the reaction time, the film system performs a metal-insulator transition combined with a structural phase transition.

The inverse reaction follows by reducing the H_1 gas pressure. This transition proved to be *reversible*. It affects the optical properties of the films by a change from metallic reflection to optical transparency.

We present, probably for the first time, the clear observation that this transition occurs reversibly in an Y-cluster system, too, at room temperature. Yet, the resulting changes of the optical properties are different since the Y clusters and also $\text{YH}_{\approx 2}$ exhibit typical resonance spectra which follow mainly Mie's theory (see Fig. 2a for theoretical spectra). For sufficiently thick cluster layers we expect the transition from yellow-red color to optical transparency.

The required atomic H_1 was produced for our samples from the added H_2 gas by depositing the Y clusters on a compact Pd film. Typical cluster sizes were 16 ± 7 nm.

Special results from our experiments are:

- The high surface to volume ratio of the clusters and their direct contact to the H_1 producing Pd surface gave

- rise to large reaction velocities towards $\text{YH}_{3-\delta}$ ($\delta \ll 1$), even at low H_2 pressures between 10^{-2} and 50 mbar.
- The inverse transition towards YH_2 is easily obtained by reducing the H_2 content. We succeeded to switch the transition of one sample (Fig. 2c) at room temperature for more than 20 times.
- In opposition to film systems, the volume expansion ($\approx 13\%$) connected with the transition does not deteriorate the stability of the cluster system because of the loose packing of the clusters.

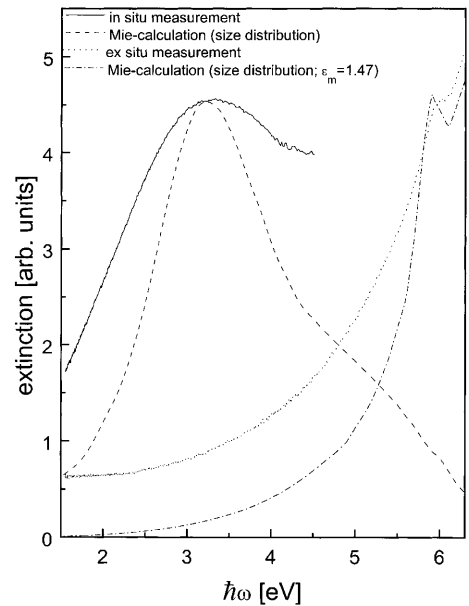


Fig. 3. Extinction measurement and Mie calculation of Y-clusters (solid and dashed curve) and of Y_2O_3 -clusters (dotted and dash-dotted curve).

- The distinct features of our optical spectra change drastically from the two-resonance spectrum of YH_2 towards a typical band edge spectrum of $\text{YH}_{3-\delta}$ ($\delta \ll 1$). This is shown in Fig. 2b. Hence, the different phases can be easily identified by optical means.
- The gap energy, which we extracted from the slope of the interband edge, amounts to $\Delta\text{YH}_{3-\delta}$ ($\delta \ll 1$) = 2.9 eV.

3.2 The irreversible reactions $\text{Y} \rightarrow \text{YH}_2$ and $\text{Y} \rightarrow \text{Y}_2\text{O}_3$

In contrast to the reversible transition $\text{YH}_2 \rightarrow \text{YH}_{3-\delta}$ the $\text{Y} \rightarrow \text{YH}_2$ reaction in the cluster system proved to be irreversible at room temperature. It induces drastic changes of the optical spectra as shown in Figs. 2a and 2b.

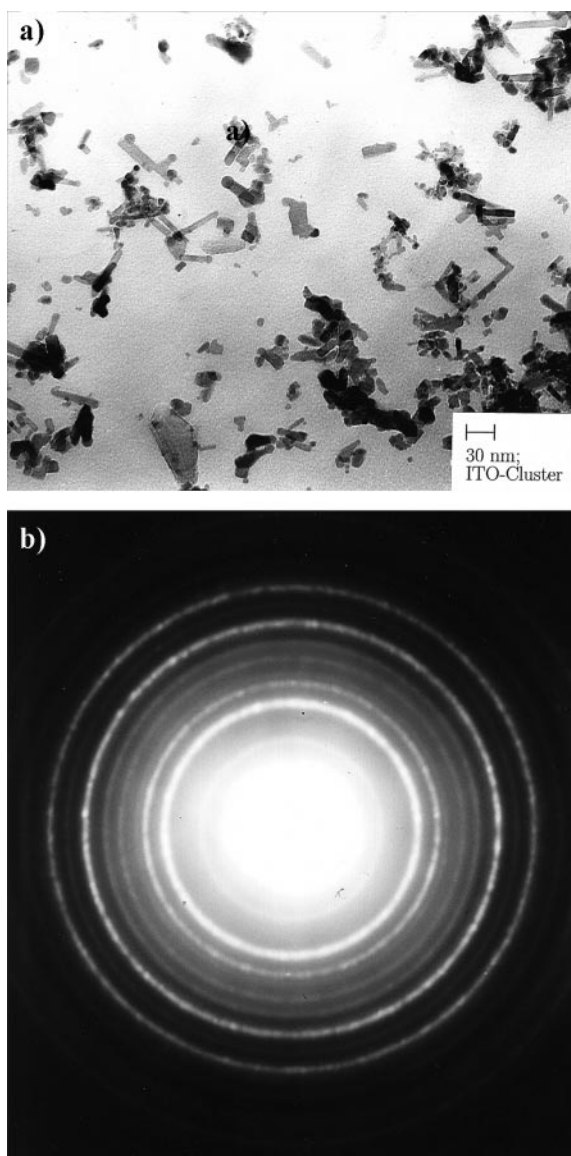


Fig. 4. (a) TEM bright-field image of ITO cluster needles. (b) Diffraction pattern of the ITO clusters. The crystallinity of the prepared cluster needles is obvious.

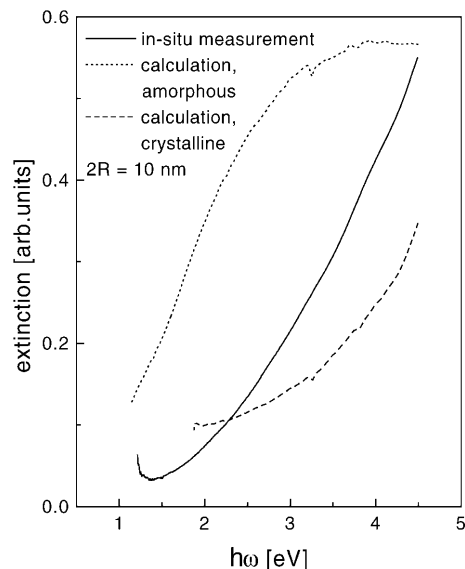


Fig. 5. Measured extinction of the ITO cluster layer is presented in comparison with calculations according to Mie's theory for spherical clusters.

Another reaction which also proved to be irreversible is the *oxidation* of the Y clusters. Again, it can be monitored by the changes of the optical absorption spectra: while Y exhibits a typical metal cluster resonance peak, spread over essential parts of the visible spectrum, the oxide is characterized by an interband transition edge in the near UV. From Fig. 3 we see how the metal cluster peak, which is probably due to a plasmon excitation, vanishes, leaving the oxide almost transparent. At 5.9 eV we resolved a tiny extra peak superimposed to the edge which is predicted by the Mie calculations.

4 Nanoporous ITO cluster layers

The high power laser source LUCAS enables us to produce crystalline Indium-Tin-Oxide (ITO) clusters from a solid target without additional annealing under oxygen. By depositing such clusters on a quartz glass substrate we produced loosely packed nanoporous cluster films. Layer thicknesses amounted up to ≈ 200 nm. Such samples are promising to incorporate additional foreign substances into the pores in order to form special kinds of composite materials.

4.1 Electron microscopical characterization

TEM analysis including bright field (Fig. 4a), dark field, diffraction (Fig. 4b) and EDX showed :

- the clusters are crystalline with preferably rod structure without any need of annealing in oxygen atmosphere,
- the cluster needles form a loose network with topological percolation,

- EDX indicated the composition of 88% In and 12% Sn (atom percent).
- typical rod thicknesses are 10 nm with their lengths varying up to ≈ 200 nm.

sputtered films exhibited $\rho \geq 7 \times 10^{-4} \Omega \text{ cm.}$) This low resistivity is promising for technical applications. It indicates the formation of good interface contacts between neighboring clusters forming a random network with stable electrical percolation.

4.2 Optical absorption measurements

The in-situ measured optical extinction of one ITO-cluster sample is shown in Fig. 5. The sample proved to be almost transparent in VIS, the slight extinction increasing towards UV. This trend approaches fairly well the spectrum calculated from Mie's theory for (spherical!) crystalline ITO clusters. The experimental spectrum differs strongly from the theoretical spectrum of *amorphous* ITO clusters also shown in Fig. 5. (The according optical material constants were measured by Maass [9]).

The samples exhibited clearly perceptible light scattering. Additionally ex-situ measured spectra differ only slightly from the in-situ spectra, hence the subsequent contact with oxygen (at room temperature) does not alter the films essentially.

4.3 Electrical measurements

The resistivity of a 190 nm thick ITO cluster film was determined by the van der Pauw method, contacting the samples directly by tips.

We found the resistivity to amount to $\rho = 9 \times 10^{-3} \Omega \text{ cm}$ at room temperature. (For comparison: 100 nm compact

References

1. U. Kreibig, A. Hilger, M. Gartz: Ber. Bunsenges. Phys. Chem. **101**, 1593 (1997)
2. U. Kreibig, M. Vollmer: *Optical Properties of Metal Clusters*, 1st edn. (Springer, Berlin 1995)
3. G.K. Wertheim, D.N.E. Buchanan: Phys. Rev. B **50**, 11070 (1994)
4. B. Lamprecht, A. Leitner, F.R. Aussenegg: Appl. Phys. B **64**, 269 (1997)
5. J. Klein-Wiehle, P. Simon, H. Rubahn: Phys. Rev. Lett. (1998) submitted
6. J.N. Huiberts, R. Griessen, J.H. Rector, K.J. Wijngaarden, J.P. Dekker, D.G. De Groot, N.J. Koeman: Lett. Nat. **380**, 21 March (1996)
7. P. van der Sluis, M. Ouwerkerk, P.A. Duine: Appl. Phys. Lett. **70**(25), 3356 (1997)
8. J.H. Weaver, R. Rosei, D.T. Peterson: Phys. Rev. B **19**(10), 4855 (1979)
9. J. Maass: Diploma work, University of Technology Aachen (1996)
10. B.N.J. Persson: Surf. Sci. **281**, 153 (1993)
11. M. Quinten, J. Rostalski: Part. Part. Syst. Charact. **13**, 89 (1996)